Available online at www.sciencedirect.com
SCIENCE DIRECT®
Physics Letters B 610 (2005) 165–176
PHYSICS LETTERS B
www.elsevier.com/locate/physletb

Search for CP violation in $K^0 \to 3\pi^0$ decays

NA48 Collaboration

A. Lai, D. Marras

Dipartimento di Fisica dell'Università e Sezione dell'INFN di Cagliari, I-09100 Cagliari, Italy

J.R. Batley, R.S. Dosanjh [1], T.J. Gershon [2], G.E. Kalmus, C. Lazzeroni, D.J. Munday, E. Olaiya [3], M.A. Parker, T.O. White, S.A. Wotton

Cavendish Laboratory, University of Cambridge, Cambridge CB3 0HE, UK [4]

R. Arcidiacono [5], G. Barr [6], G. Bocquet, A. Ceccucci, T. Cuhadar-Dönszelmann [7], D. Cundy [8], N. Doble [9], V. Falaleev, L. Gatignon, A. Gonidec, B. Gorini, P. Grafström, W. Kubischta, A. Lacourt, I. Mikulec [10], A. Norton, B. Panzer-Steindel, G. Tatishvili [11,12], H. Wahl [13]

CERN, CH-1211 Genève 23, Switzerland

C. Cheshkov [14], P. Hristov [14], V. Kekelidze, D. Madigojine, N. Molokanova, Yu. Potrebenikov, A. Zinchenko

Joint Institute for Nuclear Research, Dubna, Russia

V. Martin [15], P. Rubin [16], R. Sacco [17], A. Walker

Department of Physics and Astronomy, University of Edinburgh, JCMB King's Buildings, Mayfield Road, Edinburgh EH9 3JZ, UK

M. Contalbrigo, P. Dalpiaz, J. Duclos, M. Fiorini, P.L. Frabetti [18], A. Gianoli, M. Martini, F. Petrucci, M. Savrié

Dipartimento di Fisica dell'Università e Sezione dell'INFN di Ferrara, I-44100 Ferrara, Italy

A. Bizzeti [19], M. Calvetti, G. Collazuol [9], G. Graziani [20], E. Iacopini, M. Lenti, F. Martelli [21], M. Veltri [21]

Dipartimento di Fisica dell'Università e Sezione dell'INFN di Firenze, I-50125 Firenze, Italy

0370-2693/$ – see front matter
doi:10.1016/j.physletb.2005.01.065

K. Eppard, M. Eppard [14], A. Hirstius [14], K. Kleinknecht, U. Koch, L. Köpke, P. Lopes da Silva, P. Marouelli, I. Mestvirishvili, I. Pellmann [22], A. Peters [14], S.A. Schmidt, V. Schönharting, Y. Schué, R. Wanke, A. Winhart, M. Wittgen [23]

Institut für Physik, Universität Mainz, D-55099 Mainz, Germany [24]

J.C. Chollet, L. Fayard, L. Iconomidou-Fayard, G. Unal, I. Wingerter-Seez

Laboratoire de l'Accélérateur Linéaire, IN2P3-CNRS, Université de Paris-Sud, F-91898 Orsay, France [25]

G. Anzivino, P. Cenci, E. Imbergamo, P. Lubrano, A. Mestvirishvili [26], A. Nappi, M. Pepe, M. Piccini

Dipartimento di Fisica dell'Università e Sezione dell'INFN di Perugia, I-06100 Perugia, Italy

R. Casali, C. Cerri, M. Cirilli [14], F. Costantini, R. Fantechi, L. Fiorini, S. Giudici, I. Mannelli, G. Pierazzini, M. Sozzi

Dipartimento di Fisica, Scuola Normale Superiore e Sezione dell'INFN di Pisa, I-56100 Pisa, Italy

J.B. Cheze, M. De Beer, P. Debu, F. Derue [27], A. Formica, R. Granier de Cassagnac [28], G. Gouge, G. Marel, E. Mazzucato, B. Peyaud, R. Turlay ✠, B. Vallage

DSM/DAPNIA, CEA Saclay, F-91191 Gif-sur-Yvette, France

M. Holder, A. Maier [14], M. Ziolkowski

Fachbereich Physik, Universität Siegen, D-57068 Siegen, Germany [29]

C. Biino, N. Cartiglia, F. Marchetto, E. Menichetti, N. Pastrone

Dipartimento di Fisica Sperimentale dell'Università e Sezione dell'INFN di Torino, I-10125 Torino, Italy

J. Nassalski, E. Rondio, M. Szleper [15], W. Wislicki, S. Wronka

Soltan Institute for Nuclear Studies, Laboratory for High Energy Physics, PL-00681 Warsaw, Poland [30]

H. Dibon, M. Jeitler, M. Markytan, G. Neuhofer, M. Pernicka, A. Taurok, L. Widhalm

Österreichische Akademie der Wissenschaften, Institut für Hochenergiephysik, A-1050 Wien, Austria [31]

Received 10 August 2004; received in revised form 17 January 2005; accepted 20 January 2005

Available online 2 February 2005

Editor: W.-D. Schlatter

Abstract

Using data taken during the year 2000 with the NA48 detector at the CERN SPS, a search for the CP violating decay $K_S \to 3\pi^0$ has been performed. From a fit to the lifetime distribution of about 4.9 million reconstructed $K^0/\bar{K}^0 \to 3\pi^0$ decays, the CP violating amplitude $\eta_{000} = A(K_S \to 3\pi^0)/A(K_L \to 3\pi^0)$ has been found to be $\mathrm{Re}(\eta_{000}) = -0.002 \pm 0.011 \pm 0.015$ and $\mathrm{Im}(\eta_{000}) = -0.003 \pm 0.013 \pm 0.017$. This corresponds to an upper limit on the branching fraction of $\mathrm{Br}(K_S \to 3\pi^0) <$

7.4×10^{-7} at 90% confidence level. The result is used to improve knowledge of Re(ϵ) and the CPT violating quantity Im(δ) via the Bell–Steinberger relation.

1. Introduction

The violation of CP symmetry was discovered in 1964 in the decay of the long-lived K_L meson to two charged pions [1]. Since then, other CP violating K_L decay modes—in particular direct CP violation—and CP violation in B^0 decays have been observed. The short-lived neutral kaon K_S, too, should manifest CP violating decay amplitudes. However, due to the large width of the K_S meson, the branching ratios of CP violating K_S decays are 6 orders of magnitude smaller than the branching ratios of the main CP violating K_L decays. One unambiguous signature of CP violation in K_S decays would be the observation of the decay $K_S \to 3\pi^0$. Within the Standard Model its branching ratio is predicted to be 1.9×10^{-9}, using the measured values of the corresponding K_L decay and the CP violating parameter ϵ [2].

Since the kaon is spinless, the $3\pi^0$ final state has a well-defined CP eigenvalue of -1, when neglecting direct CP violation, and the decay $K_S \to 3\pi^0$ is CP forbidden. The CP violating parameter η_{000} is defined as the amplitude ratio

$$\eta_{000} \equiv \frac{A(K_S \to 3\pi^0)}{A(K_L \to 3\pi^0)}. \tag{1}$$

E-mail address: rainer.wanke@uni-mainz.de (R. Wanke).
[1] Present address: Department of Physics, Carleton University, Ottawa, ON, K1S 5B6, Canada.
[2] Present address: High Energy Accelerator Research Organization (KEK), Tsukuba, Japan.
[3] Present address: Rutherford Appleton Laboratory, Chilton, Didcot, Oxon OX11 0QX, UK.
[4] Funded by the UK Particle Physics and Astronomy Research Council.
[5] Present address: Massachusetts Institute of Technology, Cambridge, MA 02139-4307, USA.
[6] Present address: Department of Physics, University of Oxford, Oxford OX1 3RH, UK.
[7] Present address: University of British Columbia, Vancouver, BC, V6T 1Z1, Canada.
[8] Present address: Istituto di Cosmogeofisica del CNR di Torino, I-10133 Torino, Italy.
[9] Present address: Dipartimento di Fisica, Scuola Normale Superiore e Sezione dell'INFN di Pisa, I-56100 Pisa, Italy.
[10] On leave from Österreichische Akademie der Wissenschaften, Institut für Hochenergiephysik, A-1050 Wien, Austria.
[11] On leave from Joint Institute for Nuclear Research, Dubna 141980, Russia.
[12] Present address: Carnegie Mellon University, Pittsburgh, PE 15213, USA.
[13] Present address: Dipartimento di Fisica dell'Università e Sezione dell'INFN di Ferrara, I-44100 Ferrara, Italy.
[14] Present address: CERN, CH-1211 Genève 23, Switzerland.
[15] Present address: Northwestern University, Department of Physics and Astronomy, Evanston, IL 60208, USA.
[16] Present address: Department of Physics and Astronomy, George Mason University, Fairfax, VA 22030, USA; funded by US NSF under grants 9971970 and 0140230.
[17] Present address: Department of Physics, Queen Mary University, London E1 4NS, UK.
[18] Present address: Joint Institute for Nuclear Research, Dubna 141980, Russia.
[19] Dipartimento di Fisica dell'Università di Modena e Reggio Emilia, I-41100 Modena, Italy.
[20] Present address: DSM/DAPNIA, CEA Saclay, F-91191 Gif-sur-Yvette, France.
[21] Istituto di Fisica dell'Università di Urbino, I-61029 Urbino, Italy.
[22] Present address: DESY Hamburg, D-22607 Hamburg, Germany.
[23] Present address: SLAC, Stanford, CA 94025, USA.
[24] Funded by the German Federal Minister for Research and Technology (BMBF) under contract 7MZ18P(4)-TP2.
[25] Funded by Institut National de Physique des Particules et de Physique Nucléaire (IN2P3), France.
[26] Present address: Department of Physics and Astronomy, University of Iowa, Iowa City, IA 52242-1479, USA.
[27] Present address: Laboratoire de l'Accélérateur Linéaire, IN2P3-CNRS, Université de Paris-Sud, F-91898 Orsay, France.
[28] Present address: Laboratoire Leprince-Ringuet, Ecole polytechnique/IN2P3, F-91128 Palaiseau, France.
[29] Funded by the German Federal Minister for Research and Technology (BMBF) under contract 056SI74.
[30] Supported by the Committee for Scientific Research grants 5P03B10120, SPUB-M/CERN/P03/DZ210/2000 and SPB/CERN/P03/DZ146/2002.
[31] Funded by the Austrian Ministry for Traffic and Research under the contract GZ 616.360/2-IV GZ 616.363/2-VIII, and by the Fonds für Wissenschaft und Forschung FWF Nr. P08929-PHY.
✠ Deceased.

When assuming CPT conservation and neglecting isospin $I = 3$ and non-symmetric $I = 1$ final states, $\eta_{000} = \epsilon + i\,\mathrm{Im}(A_1)/\mathrm{Re}(A_1)$ with the parameter ϵ of indirect CP violation and the $I = 1$ amplitude A_1. The imaginary part of η_{000} is in principle sensitive to direct CP violation [2].

Additional interest in $K_S \to 3\pi^0$ decays arises from the search for CPT violation. The Bell–Steinberger relation [3] links possible CPT violation in the $K^0\bar{K}^0$ mixing matrix with CP violating amplitudes in K_L and K_S decays via the conservation of probability. At present, the limit on CPT violation is limited by poor knowledge of η_{000}.

In a recent investigation, the CPLEAR experiment found $\mathrm{Re}(\eta_{000}) = 0.18 \pm 0.15$ and $\mathrm{Im}(\eta_{000}) = 0.15 \pm 0.20$ in the decay of flavour-tagged K^0 and $\bar{K}^0$ mesons [4], which corresponds to an upper bound of $\mathrm{Br}(K_S \to 3\pi^0) < 1.9 \times 10^{-5}$ at 90% confidence level. In addition, the SND Collaboration has set a limit of $\mathrm{Br}(K_S \to 3\pi^0) < 1.4 \times 10^{-5}$ [5].

In this Letter we report an improved measurement of the η_{000} parameter using data collected from a short neutral beam with the NA48 detector at CERN. Sensitivity to η_{000} comes from $K_S/K_L \to 3\pi^0$ interference at small decay times near the target. A beam of pure K_L decays, taken under the same experimental conditions, was used for normalization. The experimental set-up is described in Section 2, while Section 3 deals with event selection and reconstruction. The fit to extract the parameter η_{000} is described in Section 4. Section 5 discusses the implications of the result with respect to the $K_S \to 3\pi^0$ branching fraction and the limit on CPT violation.

2. Experimental setup

The NA48 experiment was designed for the measurement of direct CP violation in neutral kaon decays. Its main feature is two simultaneous, almost collinear beams of neutral kaons derived from proton beams from the CERN SPS delivered to two fixed targets [6]. The kaon beams have a common decay region and decays from both beams are recorded with the same detector (see Fig. 1). Both targets are made from beryllium and have a length of 400 mm and a diameter of 2 mm. The far target is located 126 m before the beginning of the decay region while the near target is only 6 m up-stream of the fiducial region and displaced by 7.2 cm in the vertical direction from the axis of the far-target beam. The two beam axes have an angle of 0.6 mrad with respect to each other and cross at the longitudinal position of the electromagnetic calorimeter, 120 m down-stream of the near target. In both beams, charged particles are deflected by sweeping

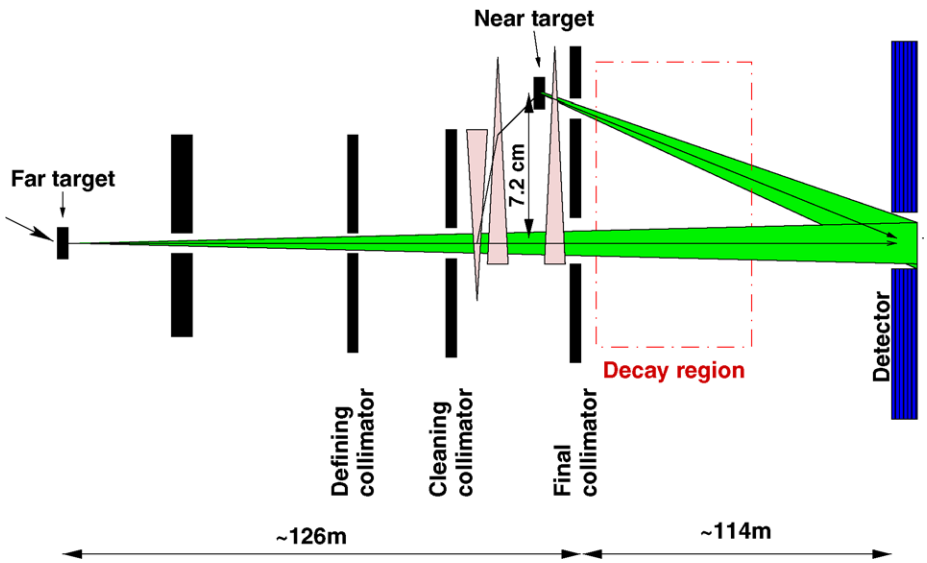

Fig. 1. Beam-line of the NA48 experiment during the 2000 data taking.

magnets. Particle decays from the far target are almost exclusively K_L decays, while decays originating from the near target are mainly K_S (and neutral hyperon) decays with, however, a small component of K_L decays.

The analysis reported here is based on data from a 40-day run period in 2000, with only the near target in operation. The neutral beam was produced by 400 GeV/c protons at a production angle of 3.0 mrad, with a beam intensity of about 10^{10} protons during a 3.2 s long SPS spill. This was about a factor of 300 higher than the typical intensity of the near-target beam during the direct CP violation measurement. This high-intensity run period was preceded by a 30-day run with only a far-target beam under the same beam conditions, except for the proton beam energy being 450 GeV and the production angle being 2.4 mrad. The data from this first run period were used for normalization purposes.

In the usual configuration, the main NA48 detector elements are a magnetic spectrometer for reconstruction of charged particles, followed by a hodoscope for charged particles and a liquid krypton electromagnetic calorimeter (LKr). During both run periods in 2000, the spectrometer drift chambers were absent and its vessel evacuated, leaving no material between the final collimator and the hodoscope for charged particles directly in front of the calorimeter. In the far-target run period, the spectrometer magnet was powered with an integrated field of 0.88 Tm in order to have the same running conditions for systematic studies of the direct CP violation measurement. In the subsequent near-target run period the magnet was off.

The liquid krypton calorimeter measures the energies, positions, and times of electromagnetic showers initiated by photons and electrons [7]. It has a length of 127 cm, corresponding to 27 radiation lengths, and consists of 13212 cells in a projective tower geometry which points to the middle of the decay volume. The active volume has an octagonal shaped cross section of about 5.5 m^2. Each cell has a 2×2 cm^2 cross section and is formed by copper-beryllium ribbons which are extended longitudinally in a ± 48 mrad accordion structure. The cells are contained in a cryostat filled with about 10 m^3 of liquid krypton at a temperature of 120 K. The initial ionization signal induced on the electrodes is amplified, shaped, and digitized by 40 MHz FADCs. The energy resolution of the calorimeter was

$$\frac{\sigma(E)}{E} \simeq \frac{0.090}{E} \oplus \frac{0.032}{\sqrt{E}} \oplus 0.0042 \qquad (2)$$

with E in GeV. The spatial and time resolutions were better than 1.3 mm and 300 ps, respectively, for a photon with energy above 20 GeV. The read-out system was calibrated by a charge pulse every burst during data taking. The relative calibration of the individual cells was determined by using K_{e3} decays during the 1998 run period and checked to be similar in 2000 by $\pi^0/\eta \to \gamma\gamma$ decays produced in thin plastic targets in a special run with a π^- beam. The final calibration of the overall energy scale was performed by fitting the effective edge of the collimator as reconstructed in the data to the one in the Monte Carlo simulation.

The hadron calorimeter follows the LKr calorimeter and was used as a veto-counter. It is composed of forty-eight 24 mm thick steel plates interleaved with scintillator plates and measures energies and horizontal and vertical positions of hadronic showers. A more complete description of the NA48 detector can be found in Ref. [8].

The trigger decision for $3\pi^0$ events was based on projections of the deposited energy in the liquid krypton calorimeter [9]. In both run periods the trigger required a total deposited energy of at least 50 GeV. In addition, the radius of the energy centre-of-gravity had to be less than 15 cm from the detector axis and the proper kaon lifetime, measured from the final collimator, had to be less than 9 K_S lifetimes with both radius and proper lifetime computed online from the moments of the energy depositions in the calorimeter. The trigger efficiency was determined using a $3\pi^0$ data sample triggered by a scintillating fiber hodoscope located inside the calorimeter. It was measured to be 99.8% in both the near- and the far-target run periods, and showed no dependence on energy or decay vertex position within the decay volume used in the analysis.

3. Event selection and reconstruction

To identify $K^0 \to 3\pi^0 \to 6\gamma$ events and to determine their kinematics, the measured energies E_i, positions x_i and y_i, and times of the photon showers in the liquid krypton electromagnetic calorimeter are used.

From the energies deposited in the LKr cells, clusters were formed, which had to fulfill the following selection criteria. The cluster energies were required to be above 3 GeV and below 100 GeV, within the range of the linear energy response of the calorimeter. To avoid energy losses, each cluster had to be more than 5 cm from the edge of the beam pipe and from the outer edge of the sensitive area. In addition, the distance to the closest dead cell of the calorimeter was required to be larger than 2 cm.

On all combinations of 6 clusters which passed these requirements, the following further selection criteria were applied. To avoid difficulties with the sharing of energy among close clusters, the minimum distance between two clusters had to be at least 10 cm. All six clusters were required to lie within 2 ns of the average cluster time. The sum of cluster energies had to lie above 60 GeV and below 185 GeV. The radial position r_{cog} of the energy centre-of-gravity at the calorimeter had to be less than 7 cm in the near-target and less than 4 cm in the far-target run, which had stronger beam collimation.

To avoid background from accidental pile-up, events with more than one such combination of clusters and those with additional clusters with an energy above 1.5 GeV within 3 ns of the event time were rejected.

From the surviving candidates, the longitudinal vertex along the z direction was reconstructed from all pairings by assuming the decay of a K^0 with the nominal mass m_K:

$$z_{\mathrm{vertex}} = z_{\mathrm{LKr}} - \frac{1}{m_K} \times \sqrt{\sum_{i=1}^{6}\sum_{j>i}^{6} E_i E_j \left[(x_i - x_j)^2 + (y_i - y_j)^2\right]} \tag{3}$$

with the distance z_{LKr} between the near target and the calorimeter. The resolution of the reconstructed longitudinal vertex position is about 60 cm, corresponding to ~ 0.1 K_S lifetimes for typical kaon energies.

Using the longitudinal vertex position z_{vertex}, the invariant two-photon masses m_1, m_2, and m_3 were computed for all 15 possible photon pairing combinations, and a χ^2-like variable was constructed as

$$\chi^2_{3\pi^0} = \left(\frac{\frac{1}{3}(m_1+m_2+m_3) - m_{\pi^0}}{\sigma_1}\right)^2 + \left(\frac{\frac{1}{2}(m_1 - \frac{m_2+m_3}{2})}{\sigma_2}\right)^2 + \left(\frac{\frac{1}{2}(m_2-m_3)}{\sigma_3}\right)^2. \tag{4}$$

The resolutions σ_i, parameterized as a function of the smallest photon energy, were determined from data. The mass combinations entering the individual terms are to a good approximation uncorrelated. The combination with the lowest value of $\chi^2_{3\pi^0}$ was chosen. In addition, a value of $\chi^2_{3\pi^0}$ less than 90 was required for this combination.

To reject possible background from hadrons, we required the total energy deposited in the hadron calorimeter within 15 ns of the event time to be less than 3 GeV, which removed 0.15% of the signal events.

The z_{vertex} and energy distributions of the selected events are shown in Figs. 2 and 3. For the fit of the parameter η_{000}, only events with a longitudinal vertex position $z_{\mathrm{vertex}} > 8$ m were considered to avoid detector resolution effects for vertex positions near the final collimator at $z = 6$ m. The down-stream vertex region was limited by $z_{\mathrm{vertex}} < 55$ m and a maximum lifetime of $8\tau_{K_S}$. In addition, events with lifetimes $t_{\mathrm{coll}}/\tau_{K_S} > 0.8 + 0.06 \times E_K/\mathrm{GeV}$, measured from the final collimator, were rejected to avoid a region at low energies and high lifetimes where the trigger was partly inefficient. The accepted region in proper time and energy is shown in Fig. 4.

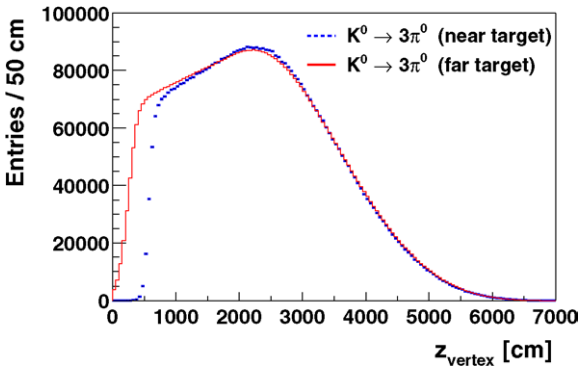

Fig. 2. Longitudinal vertex position of reconstructed $K^0 \to 3\pi^0$ events. In the figure, the far-target data have been normalized to the near-target data in the fiducial decay region.

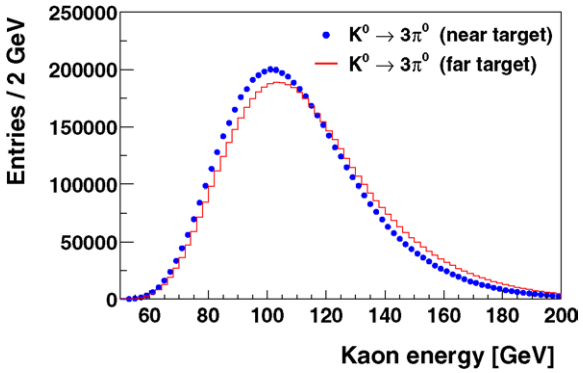

Fig. 3. Energy spectra of reconstructed $K^0 \to 3\pi^0$ events. The far-target data have been normalized to the near-target data.

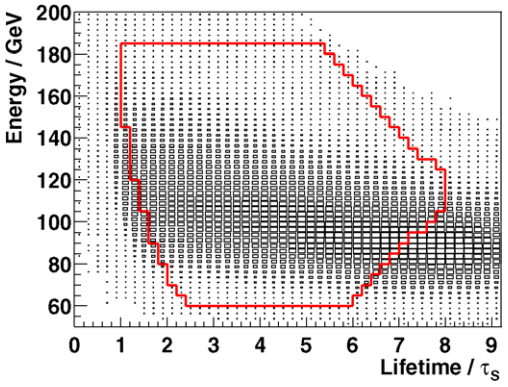

Fig. 4. Energy versus lifetime, measured from the target, of accepted $K \to 3\pi^0$ events from the near-target run. The contour encloses the accepted region for the η_{000} fit.

In total, about 4.9×10^6 $K_{L,S} \to 3\pi^0$ events were reconstructed from the data of the near-target run and about 109×10^6 $K_L \to 3\pi^0$ events from the far-target run data.

4. Data analysis

4.1. Method of the measurement

At the targets, K_L and K_S mesons are produced by strong interactions in equal amounts. The $K \to 3\pi^0$ intensity as a function of proper time t, measured from the target, is then given by

$$I_{3\pi^0}(t) \propto e^{-\Gamma_L t} + |\eta_{000}|^2 e^{-\Gamma_S t} + 2D(p)\big[\mathrm{Re}(\eta_{000})\cos(\Delta m t) - \mathrm{Im}(\eta_{000})\sin(\Delta m t)\big] e^{-\frac{1}{2}(\Gamma_S+\Gamma_L)t} \quad (5)$$

with the total K_L and K_S widths Γ_L and Γ_S and the $K_L K_S$ mass difference Δm. The *dilution* $D(p) = (N_{K^0} - N_{\bar{K}^0})/(N_{K^0} + N_{\bar{K}^0})$ describes the momentum dependent production asymmetry between K^0 and $\bar{K}^0$ at the target. For the η_{000} measurement we analyzed data from the near-target run period, using the pure $K_L \to 3\pi^0$ from the immediately preceding far-target run period to correct for trigger, acceptance, and reconstruction efficiencies. The difference of the kaon beam momentum spectra between the two periods was taken into account by performing the analysis in 5 GeV wide bins of energy covering a range from 60 to 185 GeV. The two set-ups had small differences in geometry, incident kaon beam angles, and collimation. Based on Monte Carlo studies with samples of about 90 million reconstructed events for each beam, the ratio

$$f_{3\pi^0}(t) = \frac{N^{\mathrm{near}}(t)}{N^{\mathrm{far}}(t)} \Big/ \frac{\epsilon^{\mathrm{near}}(t)}{\epsilon^{\mathrm{far}}(t)} \quad (6)$$

with the numbers N^{near} and N^{far} of reconstructed events and the acceptances ϵ^{near} and ϵ^{far} for near and far targets was determined. The geometrical correction $\epsilon^{\mathrm{near}}(t)/\epsilon^{\mathrm{far}}(t)$ between the two beams nearly equals to 1 and is shown in Fig. 5 for three different energy intervals. Neglecting this correction would shift the η_{000} result by $\Delta\,\mathrm{Re}(\eta_{000}) = -0.03$ and $\Delta\,\mathrm{Im}(\eta_{000}) = 0.03$.

The intensity $I_{3\pi^0}(t)$ as function of proper time might be altered if there is significant K_S regeneration by K_L mesons hitting the final collimator. This possibility has been considered and found to be negligible for the measurement presented here.

In the near-target data decays $K \to \pi^0\pi^0\pi^0_D$ with one pion undergoing a Dalitz decay $\pi^0_D \to e^+e^-\gamma$ had to be taken into account. Since one shower could have missed the detector or could have had an energy below the detection limit of 1.5 GeV, these decays could be mis-identified as $K \to 3\pi^0 \to 6\gamma$ events. In many such cases, due to the energy loss, the decay vertex position z_{vertex} was reconstructed further down-stream (see Eq. (3)), leading to a shorter reconstructed lifetime. For the near-target run the mis-identification rate with respect to the acceptance of good $3\pi^0$ events was $\epsilon(2\pi^0\pi^0_D)/\epsilon(3\pi^0) \approx 40\%$, while it was negligible in the far-target run due to the presence of the magnetic field. Dalitz decays were taken into account in the Monte Carlo generation of the near-target $K_L \to 3\pi^0$ events.

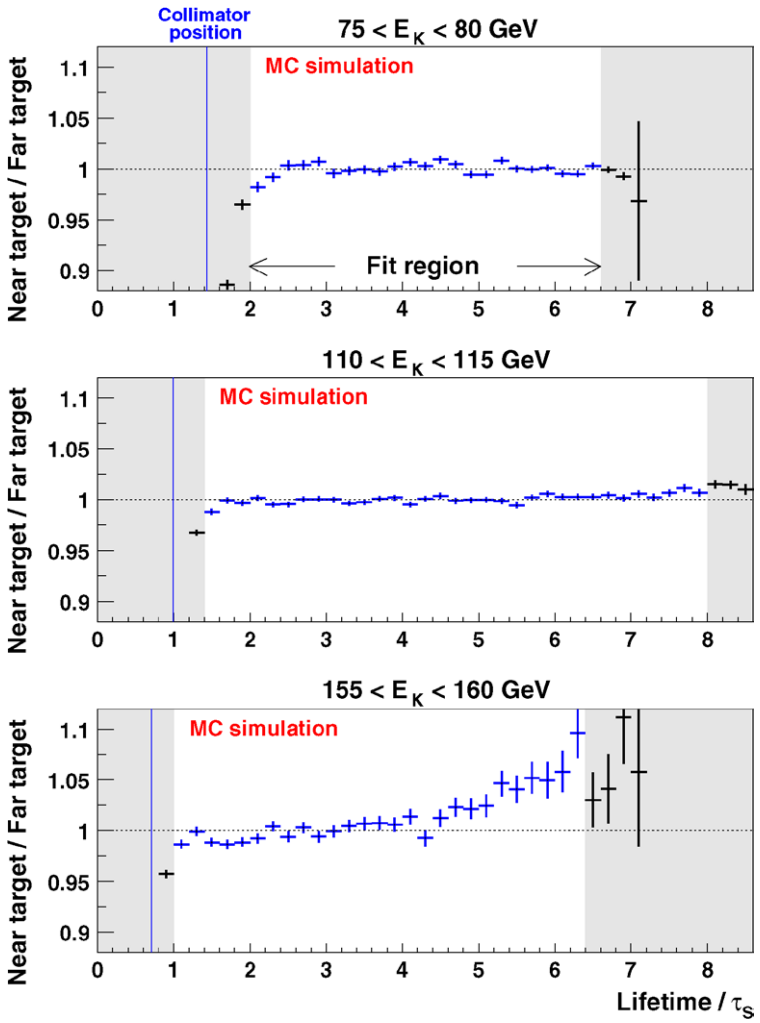

Fig. 5. Ratio $\epsilon^{\text{near}}/\epsilon^{\text{far}}$ of the acceptances for $3\pi^0$ events from the two kaon beams in three kaon energy ranges, as determined by Monte Carlo simulation.

4.2. Fit to the data

For all $K^0 \to 3\pi^0$ candidates, the proper lifetime of the kaon, measured from the position of the near target at $z = 0$, is computed as $t = z_{\text{vertex}}/(\gamma\beta c) \approx z_{\text{vertex}} m_K/(E_K c)$, where m_K is the kaon mass taken from the PDG and E_K is the sum of the cluster energies.

A global least-squares fit to the time evolution $I_{3\pi^0}(t)$ (Eq. (5)) is performed on the corrected time distributions $f_{3\pi^0}(t)$ (Eq. (6)) for each kaon energy interval. Free parameters in the fit are $\text{Re}(\eta_{000})$, $\text{Im}(\eta_{000})$, and the normalization constants of each energy interval. The $K^0\bar{K}^0$ dilution is assumed to be linearly dependent on energy. It is obtained using data from the NA31 experiment [10], corrected for the different momentum spectrum and production angle [11] and parameterized as $D = 2.425 \times 10^{-3} \times E_K$ [GeV].

The result of the fit gives $\text{Re}(\eta_{000}) = -0.002 \pm 0.011$ and $\text{Im}(\eta_{000}) = -0.003 \pm 0.013$ with a correlation coefficient of 0.77 between real and imaginary parts (Fig. 6). The χ^2 of the fit is 689 with 660 degrees of freedom.

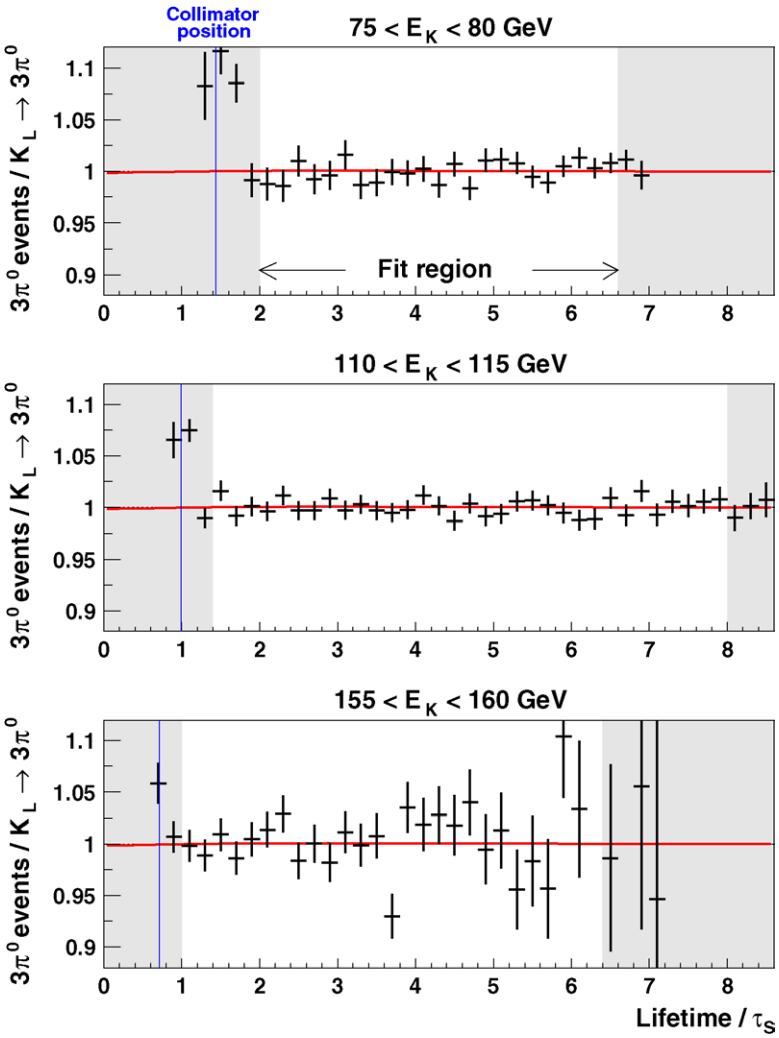

Fig. 6. The ratio of near-target over far-target $3\pi^0$ data, corrected for acceptance differences, for three different energy intervals. The points with error bars are the data. The continuous curve, which practically coincides with 1, shows the result of the fit for η_{000}.

4.3. Systematic uncertainties

We have investigated contributions to the systematic uncertainties from detector acceptance, from calorimeter energy scale and non-linearities, from possible backgrounds and accidental activity, and from $K^0\bar{K}^0$ dilution.

As described above, the acceptance determination relied on data from the far-target run, with the Monte Carlo simulation used to calculate residual geometrical differences. Many checks of the acceptance calculation were performed. Differences in the reconstruction efficiency between the two runs were investigated by varying the $\chi^2_{3\pi^0}$ cut, which led to uncertainties of $\Delta\,\mathrm{Re}(\eta_{000}) = \pm 0.009$ and $\Delta\,\mathrm{Im}(\eta_{000}) = \pm 0.013$. Remaining resolution effects near the collimator were studied by varying the up-stream vertex cut and gave an uncertainty of $\Delta\,\mathrm{Re}(\eta_{000}) = \pm 0.010$, while the imaginary part—playing a role only at larger lifetimes—was unaffected. By comparing two Monte Carlo samples with different target-collimator geometries, we estimated $\Delta\,\mathrm{Re}(\eta_{000}) = \pm 0.005$ and $\Delta\,\mathrm{Im}(\eta_{000}) = \pm 0.007$ as uncertainties related to the z_{vertex} dependence of the acceptance.

While the run-to-run variation of the calorimeter energy scale was smaller than 10^{-4}, the overall energy scale is only known to 10^{-3} in the 2000 run period.[32] By varying the energy scale within $\pm 10^{-3}$ we estimated systematic uncertainties of $\Delta\,\mathrm{Re}(\eta_{000}) \simeq \Delta\,\mathrm{Im}(\eta_{000}) \simeq \pm 0.001$. Furthermore, we investigated the effect of possible non-linearities in the shower energy reconstruction by modifying the reconstructed energy by an amount $\Delta E/E = \alpha/E + \beta E + \gamma r$, with r being the radial distance of the shower from the central detector axis. The allowed ranges of the parameters α, β, and γ were determined from studies of K_{e3}, $K \to \pi^0\pi^0$, $K^0 \to 3\pi^0$, and $\pi^0/\eta \to \gamma\gamma$ decays from older data collected in 1999, and found to be $\alpha = \pm 10$ MeV, $\beta = \pm 2 \times 10^{-5}$ GeV^{-1}, and $\gamma = \pm 10^{-5}$ cm^{-1}. When varying the constants within these ranges, the fitted value of η_{000} varied by $\Delta\,\mathrm{Re}(\eta_{000}) = \pm 0.001$ and $\Delta\,\mathrm{Im}(\eta_{000}) = \pm 0.002$.

Uncertainties in the acceptance of $K \to \pi^0\pi^0\pi^0_{\mathrm{Dalitz}}$ decays in the near-target run result in an uncertainty of $\Delta\,\mathrm{Im}(\eta_{000}) = \pm 0.001$, while the uncertainty on $\mathrm{Re}(\eta_{000})$ is less than 0.001.

Background processes which could fake a $K^0 \to 3\pi^0$ event play a role only in the near-target run, where the majority of decays comes from K_S mesons and Λ and Ξ^0 hyperons. To estimate the possible background in the $K^0 \to 3\pi^0$ near-target data sample, we compared the tails of the r_{cog} distributions of $K^0 \to 3\pi^0$ events and $K_S \to \pi^0\pi^0$ events, which are practically background-free, and found no significant discrepancy (Fig. 7). Pile-up events could either fake $K^0 \to 3\pi^0$ events or lead to accidental losses due to the cut on the number of clusters in the calorimeter. From studying time side-bands and cluster widths, we found no indication for pile-up events. Events coming from $K_S \to \pi^0\pi^0$ decays, with possible π^0 Dalitz decays, fail the $\chi^2_{3\pi^0}$ criterium, as has been checked by Monte Carlo simulation. A conservative upper limit on the effect of possible background and accidental losses in the near-target beam was estimated by loosening the cuts on the energy in the hadron calorimeter and the number of clusters in the LKr calorimeter, from which we found $\Delta\,\mathrm{Re}(\eta_{000}) = \pm 0.002$ and $\Delta\,\mathrm{Im}(\eta_{000}) = \pm 0.009$.

[32] In the usual configuration for the direct CP violation measurement, the beginning of the decay volume was defined by a scintillating anti-counter in the near-target beam. In 2000, this anti-counter was removed to be able to take a 300 times more intense neutral beam, and the reconstructed collimator edge was used as reference position.

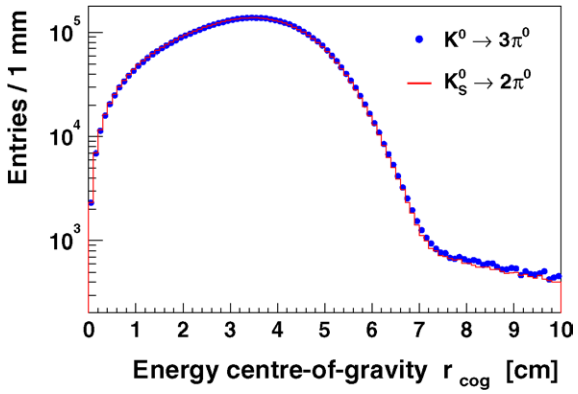

Fig. 7. Distributions of the energy centre-of gravity r_{cog} in the LKr calorimeter for reconstructed $K^0 \to 3\pi^0$ (dots) and $K_S \to \pi^0\pi^0$ (line) near-target data events. The $K_S \to \pi^0\pi^0$ events have been scaled to the number of $K^0 \to 3\pi^0$ events.

Table 1
Systematic uncertainties on the η_{000} measurement

	$\Delta\,\mathrm{Re}(\eta_{000})$	$\Delta\,\mathrm{Im}(\eta_{000})$
Reconstruction efficiency	± 0.009	± 0.013
z_{vertex} resolution	± 0.010	± 0.000
Beam geometry	± 0.005	± 0.007
Background	± 0.002	± 0.009
π^0_{Dalitz} decays	± 0.001	± 0.001
Energy scale	± 0.001	± 0.001
Energy non-linearities	± 0.001	± 0.002
$K^0\bar{K}^0$ dilution	± 0.001	± 0.001
Total	± 0.015	± 0.017

As described in the previous section, the $K^0\bar{K}^0$ dilution was taken from measured data of the NA31 experiment. By varying the dilution within the measurement errors, we obtained an uncertainty on our fit result of $|\Delta\,\mathrm{Re}(\eta_{000})| = |\Delta\,\mathrm{Im}(\eta_{000})| \leqslant 0.001$.

The systematic uncertainties for η_{000} are summarized in Table 1. The individual contributions were added in quadrature, taking correlations between $\mathrm{Re}(\eta_{000})$ and $\mathrm{Im}(\eta_{000})$ into account.

As a cross-check we have fitted the ratio $N^{\mathrm{data}}_{K_L\to 3\pi^0}(t)/N^{\mathrm{MC}}_{K_L\to 3\pi^0}(t)$ on the far-target data only. We obtained $\mathrm{Re}(\eta_{000})|_{\text{far-target}} = 0.004 \pm 0.003$ and $\mathrm{Im}(\eta_{000})|_{\text{far-target}} = -0.003 \pm 0.004$, with the result being consistent with zero, as expected.

Two additional independent analyses have been performed, yielding consistent results when applying

similar cuts. While one of these analyses employed a method similar to the one described here [12], the other analysis applied a toy Monte Carlo simulation for the geometry correction.

5. Results and discussion

Our result on η_{000} is

$$\mathrm{Re}(\eta_{000}) = -0.002 \pm 0.011(\mathrm{stat.}) \pm 0.015(\mathrm{syst.}),$$
$$\mathrm{Im}(\eta_{000}) = -0.003 \pm 0.013(\mathrm{stat.}) \pm 0.017(\mathrm{syst.}) \quad (7)$$

with a statistical correlation coefficient of 0.77 and an overall correlation coefficient of 0.57 between real and imaginary parts (Fig. 8). From this, an upper limit on the absolute value of η_{000} is obtained as

$$|\eta_{000}| < 0.045 \quad (8)$$

at the 90% confidence level. Using the measured values of $\mathrm{Br}(K_L \to 3\pi^0) = 0.211 \pm 0.003$ and of the K_L and K_S lifetimes [2], this result turns into an upper limit on the $K_S \to 3\pi^0$ branching fraction of

$$\mathrm{Br}\big(K_S \to 3\pi^0\big) = |\eta_{000}|^2 \frac{\tau_S}{\tau_L} \mathrm{Br}\big(K_L \to 3\pi^0\big) < 7.4 \times 10^{-7} \quad (9)$$

at a confidence level of 90%. This value is more than one order of magnitude below the previous best limit [5].

Under the assumptions of CPT invariance $\mathrm{Re}(\eta_{000}) \simeq \mathrm{Re}(\epsilon)$. Fixing $\mathrm{Re}(\eta_{000}) = \mathrm{Re}(\epsilon) = 1.66 \times 10^{-3}$, the fit yields $\mathrm{Im}(\eta_{000})|_{\mathrm{CPT}} = 0.000 \pm 0.009_{\mathrm{stat}} \pm 0.013_{\mathrm{syst}}$, which can be turned into upper limits of $|\eta_{000}|_{\mathrm{CPT}} < 0.025$ and $\mathrm{Br}(K_S \to 3\pi^0)|_{\mathrm{CPT}} < 2.3 \times 10^{-7}$ at a confidence level of 90%.

The result on η_{000} from the fit without imposing CPT can be used to improve the test of CPT invariance via the Bell–Steinberger relation [3]. This relation uses unitarity to connect the CP violating amplitudes of K_S and K_L decays with the CP violating parameter ϵ and the CPT violating parameter δ through

$$(1 + i \tan\phi_{\mathrm{SW}})\big[\mathrm{Re}(\epsilon) - i\,\mathrm{Im}(\delta)\big] = \sum_{\text{final states } f} A(K_L \to f)^\star A(K_S \to f)/\Gamma_S = \sum_{\text{final states } f} \alpha_f, \quad (10)$$

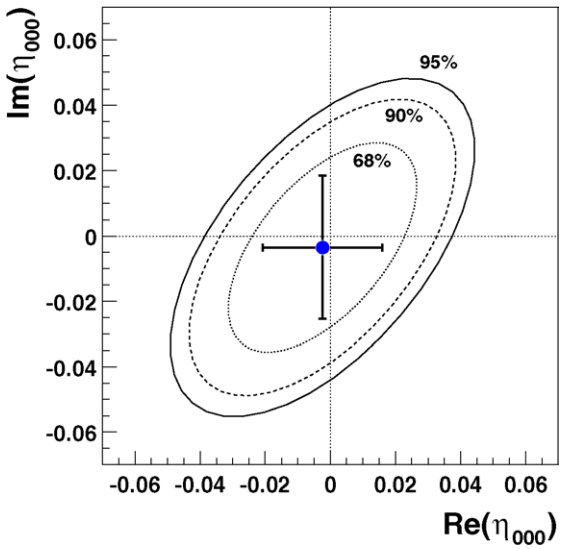

Fig. 8. Fit result for η_{000}. The errors include both statistical and systematic uncertainties. The lines indicate the exclusion limits for 68%, 90%, and 95% confidence levels.

where the super-weak angle is defined by $\tan\phi_{\mathrm{SW}} = 2(m_L - m_S)/(\Gamma_L - \Gamma_S)$. Up to now the limit on $\mathrm{Im}(\delta)$ was limited by poor knowledge of η_{000}. Together with available measurements of the other CP violating amplitude ratios (see Table 2), the K_L and K_S lifetimes, branching fractions, and mass difference [2], and the parameters $\mathrm{Re}(y)$ and $\mathrm{Im}(x_+)$ of possible CPT and $\Delta S = \Delta Q$ violation [13], the new result presented here (Eq. (7)) can be used to improve the knowledge of $\mathrm{Im}(\delta)$ and $\mathrm{Re}(\epsilon)$. Solving the complex equation (10) for the free parameters $\mathrm{Im}(\delta)$ and $\mathrm{Re}(\epsilon)$, taking into account correlations between input parameters, yields

$$\mathrm{Im}(\delta) = (-0.2 \pm 2.0) \times 10^{-5},$$
$$\mathrm{Re}(\epsilon) = (166.4 \pm 1.0) \times 10^{-5}. \quad (11)$$

The errors on both $\mathrm{Im}(\delta)$ and $\mathrm{Re}(\epsilon)$ are reduced by a factor of 2.5 with respect to the previous values [13] and are now limited by knowledge of η_{+-}.

Finally, when assuming CPT invariance in the decay, this can be converted into a measurement of the $K^0\bar{K}^0$ mass difference of

$$m_{K^0} - m_{\bar{K}^0} = (-0.2 \pm 2.8) \times 10^{-19}\ \mathrm{GeV}/c^2, \quad (12)$$

and yields an upper limit of $|m_{K^0} - m_{\bar{K}^0}| < 4.7 \times 10^{-19}\ \mathrm{GeV}/c^2$ at the 90% confidence level, which is

Table 2
Parameters $\alpha_f = A(K_L \to f)^\star A(K_S \to f)/\Gamma_S$ for decays of neutral kaons into the final state f. η_{000}, $\mathrm{Re}(\epsilon)$ and $\mathrm{Im}(\delta)$ are taken from this measurement. The $\Delta S = \Delta Q$ violating parameter $\mathrm{Im}(x_+)$ and the CPT violating parameter $\mathrm{Re}(y)$ are taken from Ref. [13]. All other measurements are from Ref. [2]

α_f	$10^3 \times \mathrm{Re}(\alpha_f)$	$10^3 \times \mathrm{Im}(\alpha_f)$
$\alpha_{+-} = \eta_{+-}\,\mathrm{Br}(K_S \to \pi^+\pi^-)$	1.146 ± 0.015	1.084 ± 0.016
$\alpha_{00} = \eta_{00}\,\mathrm{Br}(K_S \to \pi^0\pi^0)$	0.511 ± 0.008	0.488 ± 0.008
$\alpha_{+-\gamma} = \eta_{+-\gamma}\,\mathrm{Br}(K_S \to \pi^+\pi^-\gamma)$	0.003 ± 0.000	0.003 ± 0.000
$\alpha_{l3} = 2\frac{\tau_S}{\tau_L}\,\mathrm{Br}(K_L \to \pi l \nu)[\mathrm{Re}(\epsilon) - \mathrm{Re}(y) - i(\mathrm{Im}(x_+) + \mathrm{Im}(\delta))]$	0.003 ± 0.007	0.005 ± 0.006
$\alpha_{+-0} = \frac{\tau_S}{\tau_L}\eta^\star_{+-0}\,\mathrm{Br}(K_L \to \pi^+\pi^-\pi^0)$	0.000 ± 0.002	0.000 ± 0.002
$\alpha_{000} = \frac{\tau_S}{\tau_L}\eta^\star_{000}\,\mathrm{Br}(K_L \to 3\pi^0)$	-0.001 ± 0.007	0.001 ± 0.008
$\sum \alpha_f$	1.658 ± 0.024	1.581 ± 0.025

the most precise test of CPT invariance in the mass matrix.

Acknowledgements

It is a pleasure to thank the technical staff of the participating laboratories, universities, and affiliated computing centres for their efforts in the construction of the NA48 apparatus, in the operation of the experiment, and in the processing of the data.

References

[1] J.H. Christenson, J.W. Cronin, V.L. Fitch, R. Turlay, Phys. Rev. Lett. 13 (1964) 138.
[2] Particle Data Group, S. Eidelman, et al., Phys. Lett. B 592 (2004) 1.
[3] J.S. Bell, J. Steinberger, in: Proc. of Oxford Int. Conf. on Elementary Part., 1965, p. 195.
[4] CPLEAR Collaboration, A. Angelopoulos, et al., Phys. Lett. B 425 (1998) 391.
[5] SND Collaboration, M.N. Achasov, et al., Phys. Lett. B 459 (1999) 674.
[6] N. Doble, et al., Nucl. Instrum. Methods B 119 (1996) 181.
[7] G. Barr, et al., Nucl. Instrum. Methods A 370 (1996) 413.
[8] NA48 Collaboration, A. Lai, et al., Eur. Phys. J. C 22 (2001) 231.
[9] G. Barr, et al., Nucl. Instrum. Methods A 485 (2002) 676.
[10] NA31 Collaboration, R. Carosi, et al., Phys. Lett. B 237 (1990) 303.
[11] H.W. Atherton, et al., CERN Yellow Report CERN-80-07, 1980.
[12] G. Gouge, PhD thesis, DAPNIA-03-07-T, CEA/Saclay, September 2003.
[13] CPLEAR Collaboration, A. Apostolakis, et al., Phys. Lett. B 456 (1999) 297.